Received: 27 October 2025 | Accepted: 11 June 2026

DOI: 10.1111/1365-2664.70487

BRITISH ECOLOGICAL SOCIETY Journal of Applied Ecology

RESEARCH ARTICLE

High collision vulnerability of Two-banded Plovers to wind turbines revealed by GPS tracking with probabilistic altitude modelling

Erik M. Sandvig[1,2] | Sarah Saldanha[2,3] | Heraldo V. Norambuena[1,2]

[1]Centro Bahía Lomas, Facultad de Ciencias, Universidad Santo Tomás, Santiago, Chile

[2]Red de Observadores de Aves y Vida Silvestre de Chile (ROC), Santiago, Chile

[3]Institut de Recerca de la Biodiversitat (IRBio), Universitat de Barcelona, Barcelona, Spain

Correspondence
Erik M. Sandvig
Email: esandvig@santotomas.cl

Funding information
Agencia Nacional de Investigación y Desarrollo, Grant/Award Number: SIA85220018

Handling Editor: Jeremy Froidevaux

Abstract

1. Wind energy development poses collision risks to birds, yet species-specific vulnerability assessments incorporating measurement uncertainty, flight behaviour, and environmental conditions remain scarce for shorebirds.
2. We conducted the first collision vulnerability assessment for any Patagonian shorebird using GPS telemetry and a novel probabilistic approach incorporating GPS altitude measurement uncertainty. We analysed 237 flight observations from 15 Two-banded Plovers (*Anarhynchus falklandicus*) at Bahía Lomas, Chilean Patagonia, assessing collision vulnerability as the proportion of flights within the rotor swept zone under four turbine configurations. We used beta regression models incorporating GPS altitude uncertainty, flight behaviour, and meteorological conditions (wind speed and direction from ERA5 reanalysis) to identify factors influencing vulnerability.
3. Collision vulnerability ranged from 42.6% (low ground clearance: 17.34 m) to 24.6% (high clearance: 30.00 m). The best-supported models included flight speed, solar elevation, and wind direction, but not wind speed. Vulnerability varied with wind direction, peaking during winds from the northwest quadrant where median flight altitudes (~30 m) coincided with the lower rotor swept zone, and was lowest during prevailing southwesterly winds when flights remained at low altitudes (median ~ 7 m). Incorporating GPS altitude uncertainty revealed that traditional binary classification underestimates collision vulnerability by 22–44%.
4. *Synthesis and application*. Our probabilistic framework incorporating measurement uncertainty and meteorological covariates provides a template for collision vulnerability assessment applicable across taxa. Increasing turbine ground clearance reduced vulnerability by 42%. The influence of wind direction on flight altitude—and thus collision vulnerability—highlights the importance of incorporating meteorological data in collision assessments, particularly in regions with strong prevailing winds.

KEYWORDS
Anarhynchus falklandicus, collision vulnerability, ERA5 reanalysis, GPS telemetry, shorebirds, wind energy

1 | INTRODUCTION

The global renewable energy transition has accelerated wind power development worldwide, with installed capacity exceeding 1000 GW and annual growth rates of 12–15% (GWEC, 2024; IRENA, 2024). While essential for climate change mitigation, wind energy infrastructure poses threats to avian populations through direct collision mortality, habitat displacement, and barrier effects on migration routes (Drewitt & Langston, 2006; Marques et al., 2014). Annual bird mortality from wind turbines is estimated at 140,000–700,000 individuals in the United States alone, with shorebirds consistently ranking among the most vulnerable groups due to their flight behaviours, habitat preferences, and existing conservation pressures (Loss et al., 2013; Thaxter et al., 2017).

Meteorological conditions, particularly wind speed and direction, strongly influence avian flight behaviour and may modulate collision vulnerability. Birds adjust flight altitude, speed, and trajectory in response to wind conditions, with headwinds typically associated with lower flight altitudes and tailwinds with higher altitudes (Shamoun-Baranes et al., 2006; Kemp et al., 2013). These behavioural adjustments have direct implications for collision risk, as flight altitude relative to rotor swept zones (RSZs) determines exposure to turbine blades. Despite this mechanistic link, few collision vulnerability studies have incorporated meteorological covariates (Marques et al., 2014).

Shorebird populations face precipitous global declines, with 48% of species showing negative population trends (Rosenberg et al., 2019; Smith et al., 2023; Studds et al., 2017). The Charadriidae family demonstrates particular vulnerability to wind development, with documented impacts including 79–80% population reductions at operational wind farms for European Golden Plovers (*Pluvialis apricaria*) and displacement effects extending 400–500 m from turbines (Pearce-Higgins et al., 2009; Pearce-Higgins et al., 2012; Sansom et al., 2016). These impacts compound existing threats from habitat loss, climate change, and human disturbance, potentially pushing already vulnerable populations towards local extirpation (Galbraith et al., 2014).

Chilean Patagonia represents a critical frontier in global renewable energy expansion, with the Magallanes region identified as possessing world-class wind resources for green hydrogen production (Ministry of Energy, 2020; Armijo et al., 2020). Current development plans encompass over 25 GW of wind capacity across the region (Ministry of Energy, 2020), with multiple industrial-scale projects undergoing environmental assessments simultaneously. This unprecedented development scale coincides with globally important shorebird habitat supporting significant populations of endemic and near-endemic taxa such as Magellanic Plover (*Pluvianellus socialis*), Rufous-chested Dotterel (*Anarhynchus modestus*), and Two-banded Plover (*Anarhynchus falklandicus*) (Espoz et al., 2011; Imberti et al., 2023), as well as a globally important area for threatened Nearctic migrants Red Knot (*Calidris canutus rufa*) and Hudsonian Godwit (*Limosa haemastica*) (BirdLife International, 2024a, 2024b; COSEWIC, 2019; COSEWIC, 2020).

The absence of collision vulnerability data for regional and migratory shorebirds represents a fundamental gap in environmental planning that hinders established best practices for impact assessment (Josimović et al., 2021; May et al., 2017). Studies from other regions demonstrate that shorebird vulnerability varies dramatically among species, flight behaviours, and turbine configurations, making extrapolation from other taxa or regions scientifically unjustifiable (Fernández-Bellon et al., 2019; Johnston et al., 2014). Two-banded Plovers offer a valuable model to understanding regional shorebird collision vulnerability as year-round residents and intermediate body size (55–75 g) allowing GPS transmitter deployment.

Here, we provide the first GPS-based collision vulnerability assessment for any shorebird species in Patagonia. Our objectives were to: (1) quantify collision vulnerability under multiple turbine configurations using a probabilistic framework that accounts for GPS altitude uncertainty; (2) identify behavioural and meteorological factors influencing vulnerability; and (3) compare uncertainty-based estimates with traditional binary classification to evaluate methodological implications for collision vulnerability assessment.

2 | METHODS

2.1 | Study area and GPS tracking

We conducted fieldwork at Bahía Lomas, Magallanes region, Chile (52°28′08″ S, 69°22′54″ W) during November 2023 and November 2024. We deployed GPS loggers (Nano P1, 2.9 g, Druid Technology Co., Ltd.) on 29 adult Two-banded Plovers using a leg-loop harness made of 1.5 mm elastic UV and weather-resistant 'Silicone Pump Tubing' (Product 11,447, Reichelt Chemietechnik GmbH + Co). The leg loops were custom-fitted to each bird and firmly secured with a reef knot to tie off the tubing following Sanzenbacher et al. (2000) with modifications for shorebirds by Chan et al. (2016). Total tag weight including harness (3.1 g) represented 4.43 ± 0.29% of body mass, within accepted limits for shorebirds (Kenward, 2001). Devices recorded locations hourly (±3–5 m horizontal accuracy) with a BOOST function enabling higher frequency (up to 5-min intervals) when battery capacity permitted. Devices did not include accelerometers due to weight constraints. Data were downloaded remotely via Bluetooth either directly with a smartphone and the Ecotopia app or from automated HUBs deployed in the field which downloaded data from tags that are within 50–100 m radius and then relayed via the cellular network.

2.2 | Field methods

We captured adult plovers on their nest using round spring traps (RWT60, diameter 60 cm., Moudry, Czechia), using a manual trigger (~100 m reinforced fishing line) when the bird returned to incubate, capturing it as the tent claps over the nest. All birds received a unique metal alphanumerical ring on their right tarsi. We measured body mass (±0.1 g), wing chord, culmen and tarsus length and sexed birds in the field using plumage characteristics (Martínez-Piña, 2023). The complete capture, measurement, and tagging procedure lasted approximately 15–20 min per bird. Banding and GPS deployment was authorized by the Servicio Agrícola y Ganadero of Chile under permits 6610/2023 and 7069/2024. Although formal ethical approval was not required for this study, all captures, handling, and transmitter attachment followed best-practice animal welfare standards (Fair et al., 2023).

Multiple field visits between November 2023 and May 2025 were made to frequently visited foraging sites and breeding territories to search for tagged plovers to remotely download data via Bluetooth from the deployed devices with the Ecotopia app and a handheld range extender (HUB; ~100 m range). We successfully downloaded data from 19 of 29 deployed devices (66% data recovery rate), yielding 27,018 GPS locations. GPS fix counts varied among individuals (range: 127–3891 fixes; median: 1284 fixes), reflecting differences in time from deployment and data download success. The duration of fixes downloaded per individual (time between the first and last location) ranged from 14 days to 18 months. Flight observations were similarly distributed (range per individual: 2–47; median: 12; see Table S1 in Supporting Information).

2.3 | Flight behaviour classification

We classified flight behaviour using a conservative speed threshold of ≥3.0 m/s (10.8 km/h) based on radar data for Two-banded Plovers in Magallanes (Foco Ambiental & Strix, 2025). This threshold excludes walking/running behaviours while capturing all flight activities. GPS fixes with negative altitudes, impossible locations (>100 km/h movement), or obvious errors (duplicate timestamps) were excluded.

Altitude data required careful processing to account for GPS accuracy limitations and terrain variation. Raw GPS altitudes were converted to height above-ground level (AGL) using 30 m resolution digital elevation models (DEM) accessed through the *elevatr* package (Hollister et al., 2023), with estimated vertical root mean square error (RMSE) of ±10 m for terrain similar to our study area (Jenness, 2004).

2.4 | Covariates

We extracted hourly 10-m wind data (u and v components) from ERA5 reanalysis (Copernicus Climate Data Store; Hersbach et al., 2020) matched to each GPS fix location and timestamp. Wind speed was calculated as $\sqrt{(u^2 + v^2)}$. Wind direction was decomposed into sine (east–west) and cosine (north–south) components to appropriately model circular variables (Pewsey et al., 2013). Solar angle was extracted for each fix using the package *suncalc* (Thieurmel & Elmarhraoui, 2022).

2.5 | Collision vulnerability assessment

The RSZ represents the vertical airspace occupied by rotating turbine blades. The lower boundary (ground clearance) is determined by turbine hub height minus half the rotor diameter; the upper boundary equals hub height plus half the rotor diameter. We assessed collision vulnerability as the proportion of flight observations occurring within the RSZ (Band et al., 2007; Johnston et al., 2014). This metric quantifies exposure to potential collision rather than collision probability per se, which would additionally require estimates of turbine encounter rates, avoidance behaviour, and conditional collision probability given RSZ transit. Four turbine configurations were derived from environmental impact assessments of three green hydrogen projects under development in Magallanes (Table 1; Figure 1).

TABLE 1 Collision vulnerability of Two-banded Plovers under different wind turbine configurations proposed for Magallanes region green hydrogen projects, accounting for GPS uncertainty.

Scenario	Ground clearance (m)	Rotor diameter (m)	RSZ range (m)	Expected flights in RSZ	Collision vulnerability (%) [95% CI]	Relative vulnerability reduction*
Low[a]	17.34	171	17.34–188.34	100.9/239	42.6 (38.4–46.5)	–
Medium-low[b]	22.50	175	22.50–197.50	80.7/239	34.0 (29.7–38.2)	20%
Medium[c]	27.34	171	27.34–198.34	65.4/239	27.6 (23.2–31.7)	25%
High[d]	30.00	171	30.00–201.00	58.4/239	24.6 (20.3–28.8)	42%

Note: Projects and reference:
[a]H2-Magallanes, Phase 1, Foco Ambiental and Strix, 2025.
[b]HNHEnergy, GAC, 2024.
[c]H2-Magallanes, Phase 2, Foco Ambiental and Strix, 2025.
[d]Faro del Sur, Geobiota, 2025.
*Relative to low clearance scenario.

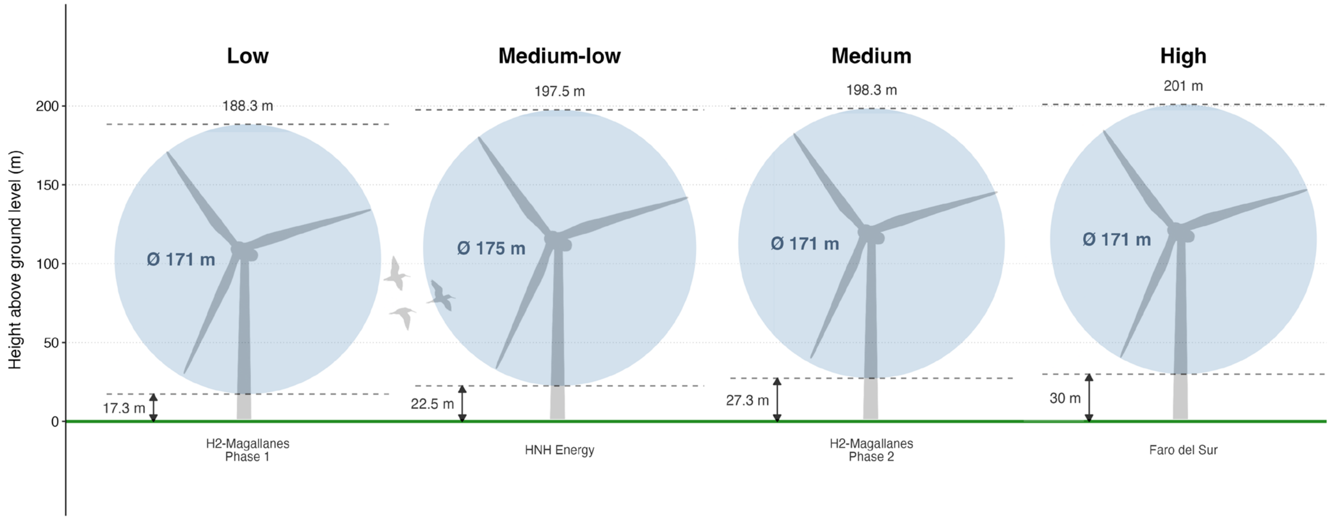

FIGURE 1 Schematic diagram of the four wind turbine configurations assessed in this study, showing ground clearance heights, rotor diameters, and rotor swept zone (RSZ) extents for each scenario derived from environmental impact assessments of green hydrogen projects proposed for Magallanes, Chile.

2.5.1 | Accounting for GPS altitude uncertainty

GPS altitude measurements contain inherent vertical uncertainty that varies with satellite geometry. Each GPS fix includes a vertical dilution of precision (VDOP) value quantifying this uncertainty. Rather than treating altitude measurements as perfectly accurate, we incorporated measurement uncertainty into collision vulnerability estimates using a probabilistic approach.

We calculated vertical uncertainty for each fix as VDOP × 5 m (user equivalent range error), where 5 m represents the midpoint of published ranges for civilian GPS (3–7 m; D'Eon et al., 2002; Recio et al., 2011), combined with DEM uncertainty (±10 m for 30 m resolution), estimated from published RMSE values for DEM data in similar terrain (Jenness, 2004), to yield total AGL uncertainty of approximately ±14–22 m depending on satellite geometry. For each flight observation, we calculated the probability of actual altitude falling within the RSZ given this uncertainty, assuming normally distributed measurement error.

We calculated collision vulnerability as the mean probability across all flight observations, representing the expected proportion of flights within RSZ accounting for measurement uncertainty. Confidence intervals were estimated using bootstrap resampling (1000 iterations). This probabilistic method provides more robust vulnerability estimates than binary classification, particularly for flights near RSZ boundaries where measurement uncertainty can substantially affect classification. Traditional binary classification (treating each altitude measurement as exact) was calculated for comparison with our probabilistic approach (see Table S2 in Supporting Information).

2.6 | Statistical analysis

We employed beta regression within a generalized linear mixed model framework using the *glmmTMB* package (Brooks et al., 2017) to examine factors influencing collision vulnerability. We used the continuous probability values (0–1) from our uncertainty-based collision vulnerability assessment (Section 2.4) as the response variable. This approach fully utilizes probabilistic information and appropriately weights observations based on their position relative to RSZ boundaries and measurement uncertainty. We used a logit link function, making coefficients directly interpretable on the log-odds scale. Probabilities of exactly 0 or 1 were adjusted to 0.001 and 0.999 respectively to meet beta distribution requirements.

Initial diagnostic tests revealed temporal autocorrelation (Durbin-Watson = 1.72, $p = 0.042$), necessitating incorporation of an autoregressive correlation structure (AR1) to account for non-independence of consecutive observations from the same individual. Candidate predictors included flight speed, solar elevation angle (linear and quadratic terms), wind speed, and wind direction components (sine and cosine). We compared all combinations of these predictors using AIC and likelihood ratio tests (see Table S3 in Supporting Information), selecting the best-supported model for each turbine scenario.

To evaluate whether collision vulnerability was better explained by wind direction relative to each bird's heading rather than absolute wind direction, we additionally computed flight-referenced wind components by projecting the wind vector onto the bird's flight vector (derived from GPS speed and course). This yielded a tailwind/headwind component (parallel to the flight path) and a crosswind component (perpendicular to it). We compared models using absolute wind direction (sine and cosine components), signed and unsigned flight-referenced components, and a categorical head-/cross-/tailwind classification.

All models included individual as a random intercept and an autoregressive (AR1) correlation structure. Continuous predictors were standardized. Model validation included simulation-based residual diagnostics using *DHARMa* (Hartig, 2026), dispersion tests,

Journal of Applied Ecology

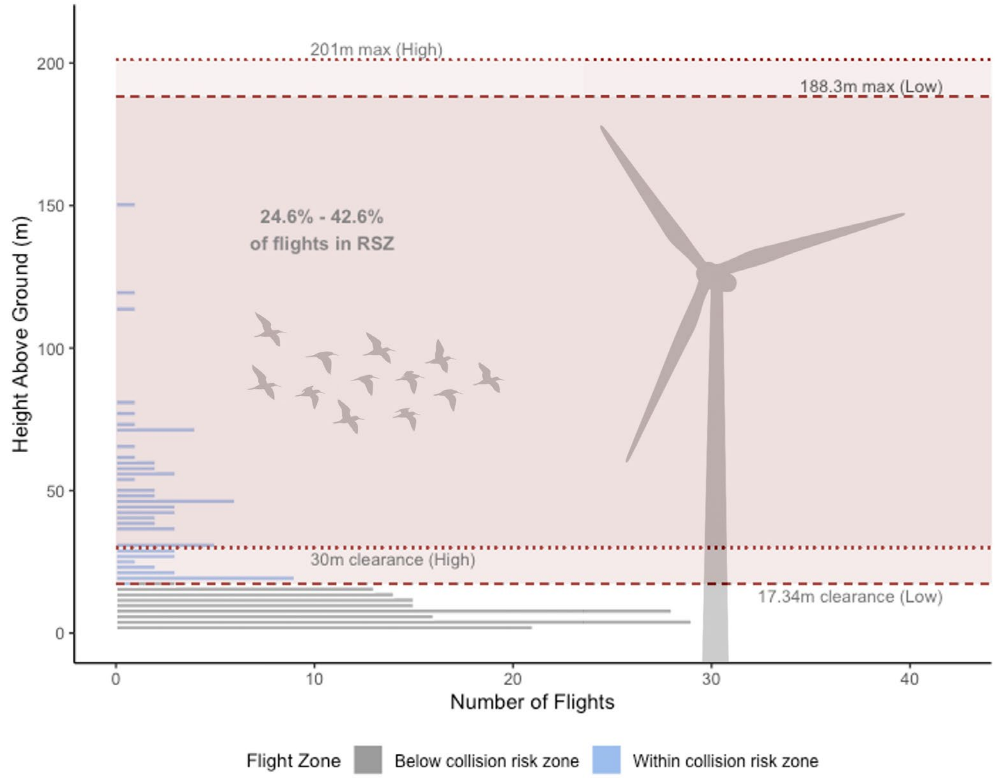

FIGURE 2 Flight altitude distribution of Two-banded Plovers ($n=237$ flights from 15 individuals) showing frequency histogram of flights below (grey) and within (blue) the extent of rotor swept zone from four turbine configurations. Shaded areas indicate rotor swept zones for Low (dashed) and High (dotted) scenarios.

and evaluation of zero-inflation. All analyses were conducted in R 4.3.2 (R Core Team, 2024).

3 | RESULTS

We obtained flight data (≥3.0 m/s) comprising 237 observations (0.9% of total fixes) from 15 of the 19 birds. Four individuals showed no GPS fixes meeting our flight speed threshold. Three had short data durations (3–7 days) with limited GPS fixes (73–152), and one had longer deployment (76 days) but yielded no flight detections. Flight altitudes showed a strongly right-skewed distribution with heights ranging from 0.1 to 418.3 m AGL (mean = 20.1 m ± 34.1 SD, median = 8.7 m; Figure 2). Flight speeds averaged 10.4 m/s (±5.0 SD, range 3.0–32.4 m/s). Speed distribution showed normal characteristics without obvious multimodality that might indicate distinct flight behaviour categories. Wind speed during flights averaged 8.4 m/s (±3.0 SD, range 1.0–15.1 m/s), with wind direction predominantly from the southwest (mean = 237°), consistent with Patagonian prevailing westerlies.

3.1 | Collision vulnerability assessment

Collision vulnerability varied significantly among turbine configurations, decreasing progressively with increasing ground clearance (Table 1). Under the lowest clearance scenario (17.34 m), 42.6% of flights (95% CI: 38.4–46.5%) occurred within the RSZ, while 24.6% (95% CI: 20.3–28.8%) occurred within RSZ under the highest clearance scenario (30.00 m)—a 42% relative reduction (Figure 2).

Traditional binary classification yielded systematically lower estimates (20.3–29.5%; Table S2), underestimating collision vulnerability by 22–44%.

3.2 | Factors influencing vulnerability

The best-supported model for the Low, Medium-low, and Medium scenarios included flight speed, solar elevation, and wind direction (sine and cosine components), but not wind speed or the quadratic solar elevation term (Table S3; AIC weights = 0.18–0.28). For the High scenario, the best-supported model included wind direction only (AIC weight = 0.32). Across all scenarios, models including wind direction received substantially greater support than models without it.

The north–south wind component (cosine) was a consistent positive predictor of collision vulnerability across all scenarios, indicating higher vulnerability with northerly wind components (Low: $\beta=0.49$, SE = 0.13, $p<0.001$; Medium-low: $\beta=0.57$, SE = 0.15, $p<0.001$; Medium: $\beta=0.33$, SE = 0.11, $p=0.002$; High: $\beta=0.33$, SE = 0.10, $p=0.002$; Table 2). The east–west component (sine) was not significant in any scenario (all $p>0.13$). Empirical examination by wind

TABLE 2 Coefficients from the best-supported beta regression models examining factors influencing collision vulnerability of Two-banded Plovers across four turbine scenarios.

	Low			Medium-low			Medium			High		
Predictor	β	SE	p	β	SE	p	β	SE	p	β	SE	p
Intercept	−0.068	0.315	0.830	−0.563	0.378	0.137	−0.569	0.248	0.022	−0.705	0.234	0.003
Flight speed	**0.269**	0.111	**0.015**	**0.339**	0.135	**0.012**	0.166	0.096	0.084	–	–	–
Solar elevation	0.223	0.116	0.053	0.239	0.141	0.089	0.177	0.100	0.077	–	–	–
Wind sin (E–W)	−0.193	0.128	0.130	−0.227	0.156	0.146	−0.144	0.110	0.190	−0.157	0.108	0.146
Wind cos (N–S)	**0.491**	0.127	**<0.001**	**0.568**	0.152	**<0.001**	**0.328**	0.107	**0.002**	**0.325**	0.104	**0.002**

Note: Coefficients are on the logit scale; significant effects ($p < 0.05$) shown in bold. Wind sin = east–west component; Wind cos = north–south component (positive values = northerly winds).

octant revealed that vulnerability was highest during winds from the northwest (mean = 0.66, n = 19), where median flight altitudes (~30 m) coincided with the lower RSZ boundary, and lowest during prevailing southwesterly winds (mean = 0.34, n = 78), where flights remained at low altitudes (median ~7 m).

Absolute wind direction explained collision vulnerability substantially better than wind direction expressed relative to the bird's flight direction. Across all four turbine scenarios, the absolute wind direction model (sine and cosine components) received the strongest support, outperforming flight-referenced formulations—including signed and unsigned tailwind/crosswind components and a categorical head-/cross-/tailwind classification—by 8–15 AIC units (see Table S4 in Supporting Information). All flight-referenced wind formulations performed worse than the base model without any wind term.

Flight speed was positively associated with vulnerability in the Low and Medium-low scenarios (β = 0.27–0.34, p = 0.012–0.015), with weaker effects at higher clearances (p = 0.084 for Medium). Solar elevation showed positive but inconsistent relationships (β = 0.18–0.24, p = 0.053–0.089; Table 2; Figure 3).

4 | DISCUSSION

4.1 | Collision vulnerability and methodological advances

Our documentation of 24.6–42.6% collision vulnerability indicates substantial exposure to potential collision from wind energy development. The predominance of low-altitude flights is consistent with recent GPS tracking of American Woodcock, where low flight altitudes explained elevated collision vulnerability (Berigan et al., 2025), suggesting low flight profiles may be a shared vulnerability trait among shorebirds.

Our probabilistic approach incorporating GPS altitude uncertainty represents a methodological advance over traditional binary classification. The 22–44% underestimation by binary methods reveals that substantial proportions of flight observations occur where measurement uncertainty overlaps with RSZ boundaries. Similarly, Johnston et al. (2023) demonstrated that flight height measurement method significantly affects collision risk estimates, underscoring the need for explicit uncertainty quantification.

The 13 percentage point difference between probabilistic (42.6%) and binary (29.5%) estimates for the Low scenario reveals that approximately 30% of flight observations occur where GPS uncertainty overlaps with the RSZ. A bird recorded at 20 ± 15 m AGL could realistically be 5–35 m, spanning both below and within the RSZ. The binary method forces an artificial yes/no decision; the probabilistic method correctly assigns partial probabilities. Our finding that ignoring measurement uncertainty underestimates collision vulnerability by 31–44% has important implications for environmental impact assessment (Péron et al., 2020; Schaub et al., 2023). Similarly, Johnston et al. (2023) demonstrated that flight height measurement method significantly affects collision risk estimates for seabirds, with GPS-derived heights yielding systematically different vulnerability estimates than barometric altimeters, underscoring the need for explicit uncertainty quantification regardless of tracking technology.

Beta regression models using probabilistic collision vulnerability as a continuous response provide methodological consistency throughout the analytical pipeline, similar to stochastic collision risk models developed for seabirds (Masden, 2015; McGregor et al., 2018). The consistency of behavioural predictors across all four turbine configurations demonstrates that conclusions are robust to both turbine design specifications and methodological approach.

4.2 | Wind direction and collision vulnerability

Wind direction, but not wind speed, was retained as a predictor in all best-supported models. Vulnerability was highest during winds from the northwest quadrant, where median flight altitudes (~30 m) coincided with the lower RSZ, and lowest during prevailing southwesterly winds (median altitude ~7 m), well below the rotor. The relative importance of wind direction increased with turbine ground clearance: for the High scenario, wind direction alone provided the best-supported model, while for lower clearance scenarios behavioural predictors (flight speed) remained influential. This indicates that at lower ground clearances, even low-altitude flights during favourable wind conditions contribute substantially to collision exposure,

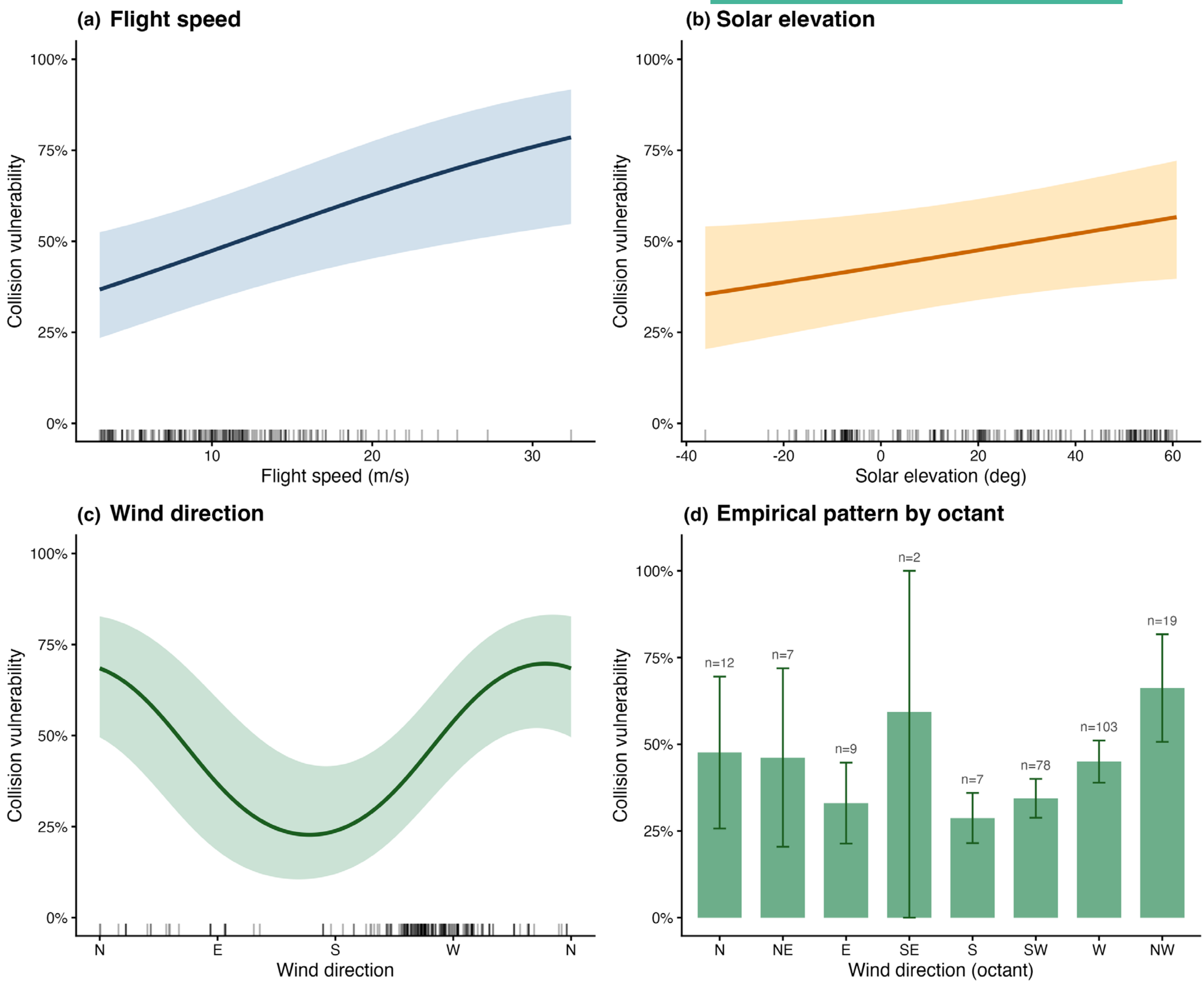

FIGURE 3 Effects of predictors on collision vulnerability of Two-banded Plovers (Low scenario, ground clearance 17.34 m). Effect of (a) flight speed; (b) solar elevation; (c) wind direction; and (d) empirical mean collision vulnerability by wind direction octant. Lines and bars show mean predictions; shaded areas show 95% confidence intervals.

whereas at higher clearances only the wind-driven climbing flights reach the rotor zone.

Notably, absolute wind direction predicted collision vulnerability better than wind direction relative to the bird's heading. This contrasts with expectations from migration studies, where birds optimize flight altitude according to the tailwind assistance they experience (Kemp et al., 2013; Shamoun-Baranes et al., 2006). The poor performance of flight-referenced wind in our system likely reflects the predominance of short commuting and foraging movements rather than sustained directional migration: for brief local flights, instantaneous wind assistance is less consequential than the broader atmospheric conditions associated with particular wind directions. Absolute wind direction may also serve as a proxy for synoptic weather states and boundary-layer dynamics—including fetch, turbulence, and orographic lift specific to this coastal site—that shape the altitudes at which birds choose to fly. These results suggest that the most informative wind metric for collision vulnerability is context-dependent: flight-referenced wind may be appropriate for migratory flights, whereas absolute wind direction better captures altitude responses during local movements. We recommend that future collision assessments evaluate both formulations, as the appropriate choice depends on the behavioural context of the flights under study.

4.3 | Behavioural patterns and mitigation

Flight speed consistently predicted collision vulnerability at lower ground clearances, with faster flights associated with increased vulnerability. Solar elevation showed weak positive relationships, indicating relatively constant vulnerability throughout daylight hours—precluding time-of-day curtailment as an effective mitigation strategy, contrasting with nocturnal migrants where nighttime curtailment achieves >90% mortality reduction (May, 2015). Recent

GPS studies demonstrate that some shorebird species exhibit avoidance of wind turbines (Schwemmer et al., 2023), though Two-banded Plover responses to operational turbines remain unknown.

Increasing ground clearance from 17.34 m to 30.00 m reduced collision vulnerability by 42%, providing immediate guidance for design optimization. However, evenoptimized designs maintain >24% vulnerability, indicating design modifications alone cannot eliminate exposure.

4.4 | Study limitations and future research

Our hourly fix interval, while typical for small shorebird deployments due to battery and weight constraints (Gould et al., 2024), presents important limitations that warrant explicit consideration. Similar constraints affect most GPS studies of shorebirds in the 50–100 g body mass range, where hourly or multi-hour fix intervals remain standard (Gould et al., 2024; Schwemmer et al., 2022). Hourly sampling likely underrepresents short-duration flights, though internal validation comparing high-interval BOOST periods to hourly sampling confirmed representative flight behaviour. Finally, our metric captures exposure but does not incorporate avoidance behaviour (Cook et al., 2014).

Our findings derive from a single site (Bahía Lomas) during two breeding seasons, limiting inference about spatial and temporal variation across the species' range. Regional extrapolation should be cautious pending multi-site studies, though the transitional habitat between steppe and coastal habitat our study covers in Bahía Lomas represents a typical scenario where multiple wind projects are proposed. Critical research priorities include: (1) multi-species vulnerability assessments; (2) displacement studies quantifying avoidance distances; (3) year-round monitoring capturing seasonal variation; (4) cumulative impact modelling integrating multiple projects; and (5) demographic modelling incorporating additional mortality from wind development.

5 | CONCLUSIONS

Our documentation of 24.6–42.6% collision vulnerability for Two-banded Plovers, accounting for GPS measurement uncertainty, demonstrates that Patagonian shorebirds face substantial exposure to potential collision from proposed wind energy development. Incorporating measurement uncertainty into collision vulnerability assessment revealed that traditional binary methods underestimate vulnerability by 31–44%, with important implications for environmental impact assessment. Increasing turbine ground clearance provides substantial vulnerability reduction (42%) but cannot eliminate exposure.

Our probabilistic framework incorporating GPS altitude uncertainty provides a template for collision vulnerability assessment applicable across taxa. We recommend: (1) adopting uncertainty-based collision vulnerability assessment as standard practice; (2) implementing higher ground clearance designs where feasible; and (3) establishing post-construction monitoring to quantify realized collision rates and avoidance behaviour.

AUTHOR CONTRIBUTIONS

Erik M. Sandvig conceived the ideas and designed methodology, with input from Heraldo V. Norambuena and Sarah Saldanha; Erik M. Sandvig, Heraldo V. Norambuena and Sarah Saldanha collected the data; Erik M. Sandvig analysed the data; Erik M. Sandvig led the writing of the manuscript. All authors contributed critically to the drafts and gave final approval for publication.

ACKNOWLEDGEMENTS

We thank the Empresa Nacional del Petróleo (ENAP) for providing logistic support and Gabriela Contreras, Pablo Galdames, Ludovica Giovinazzi, Alonso Matus, Fernando Medrano, and José Valdebenito for their assistance in fieldwork. We thank the Centro Bahia Lomas team and Dr. Fabio Labra for their ongoing support. We also are grateful to Magallanes Rovira, Eduardo Jara, Roberto Jara, and Boris Cvitanic for allowing access to the capture sites in this study.

FUNDING INFORMATION

This work was supported by the Agencia Nacional de Investigación y Desarrollo (ANID) of Chile [Subvención a la Inserción a la Academia, grant number SIA85220018].

CONFLICT OF INTEREST STATEMENT

The authors declare no conflict of interest.

DATA AVAILABILITY STATEMENT

Data and code supporting the results are available from Zenodo: https://doi.org/10.5281/zenodo.20748796 (Sandvig et al., 2026), archived from the GitHub repository https://github.com/Chilesummits/two-banded-plover-collision-vulnerability.

ORCID

Erik M. Sandvig https://orcid.org/0000-0002-4180-000X
Sarah Saldanha https://orcid.org/0000-0003-0084-1929
Heraldo V. Norambuena https://orcid.org/0000-0003-0523-3682

REFERENCES

Armijo, J., Philibert, C., & Zuloaga, P. (2020). Flexible production of green hydrogen and ammonia from variable solar and wind energy in Chile. *International Journal of Hydrogen Energy*, *45*, 1541–1558.

Band, W., Madders, M., & Whitfield, D. P. (2007). Developing field and analytical methods to assess avian collision risk at wind farms. In M. de Lucas, G. Janss, & M. Ferrer (Eds.), *Birds and wind farms*. Quercus.

Berigan, L., Clements, S., Darling, R., Fish, A., Roth, A., Balkcom, G., Carpenter, B., Costanzo, G., Duguay, J., Filkins, K., Graham, C., Harvey, W., Hook, M., Howell, D., Maddox, S., McWilliams, S., Meyer, S., Nichols, T., Pollard, J. B., … Blomberg, E. (2025). Low migratory flight altitudes may explain increased collision risk for Scolopax minor (American woodcock). *Ornithological Applications*, *127*(2), duaf017.

BirdLife International. (2024a). Calidris canutus. The IUCN Red List of Threatened Species 2024: e.T22693363A154080160. https://doi.org/10.2305/IUCN.UK.2024-2.RLTS.T22693363A154080160.en

BirdLife International. (2024b). Limosa haemastica. The IUCN Red List of Threatened Species 2024: e.T22693154A255829868. https://doi.org/10.2305/IUCN.UK.2024-2.RLTS.T22693154A255829868.en

Brooks, M., Kristensen, K., van Benthem, K., Magnusson, A., Berg, C., Nielsen, A., Skaug, H., Maechler, M., & Bolker, B. (2017). glmmTMB balances speed and flexibility among packages for zero-inflated generalized linear mixed modeling. *The R Journal*, *9*(2), 378–400. https://doi.org/10.32614/RJ-2017-066

Chan, Y. C., Brugge, M., Tibbitts, T. L., Dekinga, A., Porter, R., Klaassen, R. H., & Piersma, T. (2016). Testing an attachment method for solar-powered tracking devices on a long-distance migrating shorebird. *Journal of Ornithology*, *157*, 277–287.

Cook, A. S. C. P., Burton, N. H. K., Humphreys, E. M., & Masden, E. A. (2014). The avoidance rates of collision between birds and offshore turbines. *Scottish Marine and Freshwater Science*, *5*(16), 247. https://doi.org/10.7489/1553-1

COSEWIC. (2019). *COSEWIC assessment and status report on the Hudsonian godwit Limosa haemastica in Canada*. Committee on the Status of Endangered Wildlife in Canada.

COSEWIC. (2020). *COSEWIC assessment and status report on the red knot Calidris canutus*. Committee on the Status of Endangered Wildlife in Canada.

D'Eon, R. G., Serrouya, R., Smith, G., & Kochanny, C. O. (2002). GPS radiotelemetry error and bias in mountainous terrain. *Wildlife Society Bulletin*, *30*(2), 430–439.

Drewitt, A. L., & Langston, R. H. W. (2006). Assessing the impacts of wind farms on birds. *Ibis*, *148*, 29–42.

Espoz, C., Labra, F., Matus, R., Ponce, A., Barría, I., Saavedra, B., Figueroa, A., & Rondanelli, M. (2011). *Plan de manejo para el sitio RAMSAR Bahía Lomas*. Ministerio del Medio Ambiente/Universidad Santo Tomás/Wildlife Conservation Society.

Fair, J., Paul, E., Jones, J., & Bies, L. (Eds.). (2023). *Guidelines to the use of wild birds in research* (4th ed.). Ornithological Council.

Fernández-Bellon, D., Irwin, S., Wilson, M. W., & O'Halloran, J. (2019). Effects of development of wind energy and associated changes in land use on bird densities in upland areas. *Conservation Biology*, *33*, 413–422.

Foco Ambiental and Strix. (2025). Anexo 4-I—Evaluación de Riesgo de Colisión de Aves in Estudio de Impacto Ambiental "Proyecto de Producción de Hidrógeno y Amoníaco Verde—H2 Magallanes".

GAC. (2024). EIA—Proyecto Integral para la Producción y Exportación de Amoniaco Verde—HNH Energy, Capitulo 1, Descripción de Proyecto.

Galbraith, H., DesRochers, D. W., Brown, S., & Reed, J. M. (2014). Predicting vulnerabilities of north American shorebirds to climate change. *PLoS One*, *9*, e108899.

Geobiota. (2025). Anexo IV.3: Actualización de Evaluación de impacto ambiental de Avifauna. Adenda Estudio de Impacto Ambiental Proyecto "Parque Eólico Faro del Sur".

Gould, L. A., Manning, A. D., McGinness, H. M., & Hansen, B. D. (2024). A review of electronic devices for tracking small and medium migratory shorebirds. *Animal Biotelemetry*, *12*, 11.

GWEC (Global Wind Energy Council). (2024). *Global wind report 2024*. Brussels, Belgium.

Hartig, F. (2026). DHARMa: Residual Diagnostics for Hierarchical (Multi-Level/Mixed) Regression Models. R package version 0.5.0. https://doi.org/10.32614/CRAN.package.DHARMa

Hersbach, H., Bell, B., Berrisford, P., Hirahara, S., Horányi, A., Muñoz-Sabater, J., Nicolas, J., Peubey, C., Radu, R., Schepers, D., Simmons, A., Soci, C., Abdalla, S., Abellan, X., Balsamo, G., Bechtold, P., Biavati, G., Bidlot, J., Bonavita, M., … Thépaut, J. N. (2020). The ERA5 global reanalysis. *Quarterly Journal of the Royal Meteorological Society*, *146*(730), 1999–2049.

Hollister, J., Shah, T., Nowosad, J., Robitaille, A., Beck, M., & Johnson, M. (2023). elevatr: Access Elevation Data from Various APIs. R package version 0.99.0.

Imberti, S., Matus, R., Blank, O., & Alsina, M. L. (2023). ¿Sobreestimación poblacional de Chorlo de Magallanes Pluvianellus socialis? Nuevos antecedentes de su tamaño poblacional. *Cotinga*, *45*, 60–69.

IRENA. (2024). *Renewable energy statistics 2024*. International Renewable Energy Agency.

Jenness, J. (2004). Calculating landscape surface area from digital elevation models. *Wildlife Society Bulletin*, *32*(3), 829–839.

Johnston, A., Cook, A. S. C. P., Wright, L. J., Humphreys, E. M., & Burton, N. H. K. (2014). Modelling flight heights of marine birds to more accurately assess collision risk with offshore wind turbines. *Journal of Applied Ecology*, *51*, 31–41.

Johnston, D. T., Thaxter, C. B., Boersch-Supan, P. H., Davies, J. G., Clewley, G. D., Green, R. M. W., Shamoun-Baranes, J., Cook, A. S. C. P., Burton, N. H. K., & Humphreys, E. M. (2023). Flight heights obtained from GPS versus altimeters influence estimates of collision risk with offshore wind turbines in lesser black-backed gulls *Larus fuscus*. *Movement Ecology*, *11*(1), 66.

Josimović, B., Cvjetić, A., & Furundžić, D. (2021). Strategic environmental assessment and the precautionary principle in the spatial planning of wind farms—European experience in Serbia. *Renewable and Sustainable Energy Reviews*, *136*, 110459.

Kemp, M. U., Shamoun-Baranes, J., Dokter, A. M., van Loon, E., & Bouten, W. (2013). The influence of weather on the flight altitude of nocturnal migrants in mid-latitudes. *Ibis*, *155*(4), 734–749.

Kenward, R. E. (2001). *A manual for wildlife radio tracking* (2nd ed.). Academic Press.

Loss, S. R., Will, T., & Marra, P. P. (2013). Estimates of bird collision mortality at wind facilities in the contiguous United States. *Biological Conservation*, *168*, 201–209.

Marques, A. T., Batalha, H., Rodrigues, S., Costa, H., Pereira, M. J. R., Fonseca, C., Mascarenhas, M., & Bernardino, J. (2014). Understanding bird collisions at wind farms: An updated review on the causes and possible mitigation strategies. *Biological Conservation*, *179*, 40–52.

Martínez-Piña, D. (2023). *Aves de Chile: Guía de Campo* (p. 469). Museo Ediciones.

Masden, E. (2015). *Developing an avian collision risk model to incorporate variability and uncertainty*. Scottish Marine and Freshwater Science Vol 6 No 14 (p. 43). Scottish Government.

May, R. (2015). A unifying framework for the underlying mechanisms of avian avoidance of wind turbines. *Biological Conservation*, *190*, 179–187.

May, R., Reitan, O., Bevanger, K., Lorentsen, S. H., & Nygård, T. (2017). Mitigating wind-turbine induced avian mortality: Sensory, aerodynamic and cognitive constraints and options. *Renewable and Sustainable Energy Reviews*, *42*, 170–181.

McGregor, R. M., King, S., Donovan, C. R., Caneco, B., & Webb, A. (2018). A Stochastic Collision Risk Model for Seabirds in Flight. Marine Scotland Science Report HC0010-400-001. 61 pp.

Ministry of Energy. (2020). National Green Hydrogen Strategy—Chile. https://energia.gob.cl/sites/default/files/national_green_hydrogen_strategy_-_chile.pdf

Pearce-Higgins, J. W., Stephen, L., Douse, A., & Langston, R. H. W. (2012). Greater impacts of wind farms on bird populations during construction than subsequent operation: Results of a multi-site and multi-species analysis. *Journal of Applied Ecology*, *49*, 386–394.

Pearce-Higgins, J. W., Stephen, L., Langston, R. H. W., Bainbridge, I. P., & Bullman, R. (2009). The distribution of breeding birds around upland wind farms. *Journal of Applied Ecology*, *46*, 1323–1331.

Péron, G., Calabrese, J. M., Duriez, O., Fleming, C. H., García-Jiménez, R., Johnston, A., Safi, K., & Kays, R. (2020). The challenges of estimating the distribution of flight heights from telemetry or altimetry data. *Animal Biotelemetry*, *8*, 5.

Pewsey, A., Neuhäuser, M., & Ruxton, G. D. (2013). *Circular statistics in R*. Oxford University Press.
R Core Team. (2024). *R: A language and environment for statistical computing*. R Foundation for Statistical Computing.
Recio, M. R., Mathieu, R., Denys, P., Sirguey, P., & Seddon, P. J. (2011). Lightweight GPS-tags, one giant leap for wildlife tracking? An assessment approach. *PLoS One*, *6*(12), e28225.
Rosenberg, K. V., Dokter, A. M., Blancher, P. J., Sauer, J. R., Smith, A. C., Smith, P. A., Stanton, J. C., Panjabi, A., Helft, L., Parr, M., & Marra, P. P. (2019). Decline of the north American avifauna. *Science*, *366*(6461), 120–124.
Sandvig, E. M., Saldanha, S., & Norambuena, H. V. (2026). Data and code from: High collision vulnerability of Two-banded Plovers to wind turbines revealed by GPS tracking with probabilistic altitude modelling. Zenodo. https://doi.org/10.5281/zenodo.20748796
Sansom, A., Pearce-Higgins, J. W., & Douglas, D. J. T. (2016). Negative impact of wind energy development on a breeding shorebird assessed with a BACI study design. *Journal of Applied Ecology*, *53*, 1638–1646.
Sanzenbacher, P. M., Haig, S. M., & Oring, L. W. (2000). Application of a modified harness design for attachment of radio transmitters to shorebirds. *Wader Study Group Bulletin*, *91*, 16–20.
Schaub, T., Millon, A., De Zutter, C., Pokrovsky, I., Klaassen, R. H. G., Spiegel, O., Bretagnolle, V., & Bouten, W. (2023). How to improve the accuracy of height data from bird tracking devices? An assessment of high-frequency GPS tracking and barometric altimetry in field conditions. *Animal Biotelemetry*, *11*(1), 31.
Schwemmer, P., Mercker, M., Haecker, K., Kruckenberg, H., Kämpfer, S., Bocher, P., Fort, J., Jiguet, F., Franks, S., Elts, J., Marja, R., Piha, M., Rousseau, P., Pederson, R., Düttmann, H., Fartmann, T., & Garthe, S. (2023). Behavioral responses to offshore windfarms during migration of a declining shorebird species revealed by GPS-telemetry. *Journal of Environmental Management*, *342*, 118131.
Schwemmer, P., Mercker, M., Haecker, K., Kruckenberg, H., Kämpfer, S., Bocher, P., Fort, J., Mercker, M., Jiguet, F., Elts, J., Marja, R., Piha, M., Rousseau, P., & Garthe, S. (2022). Assessing potential conflicts between offshore wind farms and migration patterns of a threatened shorebird species. *Animal Conservation*, *26*(2), 277–291.
Shamoun-Baranes, J., van Loon, E., van Gasteren, H., van Belle, J., Bouten, W., & Buurma, L. (2006). A comparative analysis of the influence of weather on the flight altitudes of birds. *Bulletin of the American Meteorological Society*, *87*, 47–61.
Smith, P. A., Smith, A. C., Andres, B., Francis, C. M., Harrington, B., Friis, C., Morrison, R. I. G., Paquet, J., Winn, B., & Brown, S. (2023). Accelerating declines of North America's shorebirds signal the need for urgent conservation action. *Ornithological Applications*, *125*, duad003.
Studds, C. E., Kendall, B. E., Murray, N. J., Wilson, H. B., Rogers, D. I., Clemens, R. S., Gosbell, K., Hassell, C. J., Jessop, R., Melville, D. S., Milton, D. A., Minton, C. D. T., Possingham, H. P., Riegen, A. C., Straw, P., Woehler, E. J., & Fuller, R. A. (2017). Rapid population decline in migratory shorebirds relying on Yellow Sea tidal mudflats as stopover sites. *Nature Communications*, *8*, 14895.
Thaxter, C. B., Buchanan, G. M., Carr, J., Butchart, S. H. M., Newbold, T., Green, R. E., Tobias, J. A., Foden, W. B., O'Brien, S., & Pearce-Higgins, J. W. (2017). Bird and bat species' global vulnerability to collision mortality at wind farms revealed through a trait-based assessment. *Proceedings of the Royal Society B*, *284*, 20170829.
Thieurmel, B., & Elmarhraoui, A. (2022). suncalc: Compute Sun Position, Sunlight Phases, Moon Position and Lunar Phase. R package version 0.5.1.

SUPPORTING INFORMATION

Additional supporting information can be found online in the Supporting Information section at the end of this article.

Table S1. Comparison of collision vulnerability estimates using binary classification versus probabilistic methods incorporating GPS altitude uncertainty for Two-banded Plovers (*Anarhynchus falklandicus*) at Bahía Lomas, Chile ($n = 237$ flight observations from 15 individuals).

Table S2. Summary of GPS tracking data for 19 Two-banded Plovers (*Anarhynchus falklandicus*) at Bahía Lomas, Chile. Flight observations were classified as GPS fixes with instantaneous speed ≥3.0 m/s. Shaded rows indicate individuals with no detected flights.

Table S3. Comprehensive model comparison for factors influencing collision vulnerability of Two-banded Plovers across four turbine scenarios. Beta regression models were fit with individual as random intercept and AR1 temporal correlation structure. Candidate predictors: Speed = flight speed (m/s); Sun = solar elevation angle (°); Sun^2 = quadratic solar elevation; Wind speed = ERA5 10-m wind speed (m/s); Wind direction = sine and cosine components of ERA5 wind direction. k = number of estimated parameters; AIC = Akaike information criterion; ΔAIC = difference from best model; AICw = Akaike weight. Best-supported model in each scenario highlighted in green.

Table S4. Comparison of alternative wind direction formulations for modelling collision vulnerability of Two-banded Plovers across four turbine scenarios. We tested whether wind direction relative to the bird's flight direction (Course) improved model fit over absolute wind direction. Relative wind components were calculated by projecting the wind vector onto the flight vector: tailwind (positive)/headwind (negative) along the flight axis, and crosswind perpendicular to it. Categorical wind classified each flight as head-, cross-, or tailwind using 90° sectors. All models also included flight speed, solar elevation, individual random intercept, and AR1 temporal correlation. Across all scenarios, the absolute wind direction model (sine + cosine components) received the strongest support, outperforming all relative wind formulations and the base model. Best model in each scenario highlighted in green. k = parameters; ΔAIC = difference from best model.

How to cite this article: Sandvig, E. M., Saldanha, S., & Norambuena, H. V. (2026). High collision vulnerability of Two-banded Plovers to wind turbines revealed by GPS tracking with probabilistic altitude modelling. *Journal of Applied Ecology*, *63*, e70487. https://doi.org/10.1111/1365-2664.70487